Determination of the δ^2H values of high molecular weight lipids by high temperature GC coupled to isotope ratio mass spectrometry

Sabine K. Lengger[1,2*], Yuki Weber[3], Kyle W.R. Taylor[4], Sebastian H. Kopf[5], Robert Berstan[4], Ian D. Bull[1], Jan-Peter Mayser[1], William D. Leavitt[6], Jerome Blewett[1], Ann Pearson[3] and Richard D. Pancost[1,7]

1 Organic Geochemistry Unit, School of Chemistry, University of Bristol, Cantock's Close, Bristol BS81TS, UK

2 Biogeochemistry Research Centre, School of Geography, Earth and Environmental Science, University of Plymouth, Drake Circus, Plymouth PL48AA, UK

3 Department of Earth and Planetary Sciences, Harvard University, 20 Oxford St, Cambridge, MA 02138, USA

4 Elementar UK Ltd., Earl Road, Cheadle Hulme, Stockport, SK8 6PT, UK

5 Department of Geological Sciences, University of Colorado Boulder, Boulder, CO, USA

6 Department of Earth Science, Department of Chemistry, Department of Biological Sciences, Dartmouth College, Hanover, NH, USA

7 School of Earth Sciences and Cabot Institute for the Environment, University of Bristol, Queens Road, Bristol BS81RL, UK

* corresponding author: sabine.lengger@plymouth.ac.uk

Abstract

Rationale: The hydrogen isotopic composition of lipids (δ^2H_{lipid}) is widely used in food science and as a proxy for past hydrological conditions. Determining the δ^2H values of large, well-preserved triacylglycerides and other uniquely microbial lipids, such as glycerol dialkyl glycerol tetraether (GDGT) lipids, is thus of widespread interest but has so far not been

possible due to their size which prohibits analysis by traditional gas chromatography pyrolysis isotope ratio mass spectrometry (GC-P-IRMS).

Methods: We determined the δ^2H values of large, polar molecules and applied high temperature gas chromatography (GC) methods on a modified GC-P-IRMS system. The methods were validated using authentic standards of large, functionalised molecules (triacylglycerides, TAG), purified reference standards of GDGTs, and compared to δ^2H values determined by elemental analyser pyrolysis isotope ratio mass spectrometry (EA-P-IRMS); and subsequently applied to the analysis of GDGTs in a sample from a methane seep and a Welsh peat.

Results: δ^2H values of TAGs agreed within error between different between GC-P-IRMS and EA-P-IRMS, with GC-P-IRMS showing 3-5 ‰ precision for 10 ng H injected. Archaeal lipid GDGTs with up to three cyclisations could be analysed: δ^2H values were not significantly different between methods with standard deviations of 5 to 6 ‰. When environmental samples were analysed, δ^2H values of isoGDGTs were 50 ‰ more negative than those of terrestrial brGDGTs.

Conclusions: Our results indicate that the high temperature GC-P-IRMS (HTGC-P-IRMS) method developed here is appropriate to determine the δ^2H values of TAGs, GDGT lipids with up to two cyclisations, and potentially other high molecular weight compounds. The methodology will widen the current analytical window for biomarker and alimentary light stable isotope analyses. Moreover, our initial measurements suggest that bacterial and archaeal GDGT δ^2H values can record environmental and ecological conditions.

Introduction

The stable hydrogen isotopic composition (δ^2H values) of water varies systematically across the globe [1–3]. The δ^2H values of biological molecules, in turn, are dependent on the δ^2H of the H_2O available to the producing organism (source water), overprinted by biochemical processes. δ^2H values of bulk organic matter and individual compounds are used across a range of disciplines, e.g., in ecology and biology to trace animal migration patterns and foodwebs [4,5], in forensic science to identify geographical origins of victims or suspects [6], and in food science to determine the provenance of products such as honey [7], milk [8], and meat [9]. The determination of δ^2H values has also resulted in substantial discoveries in archaeology, such as the earliest horse milking [10], or manuring practices [11], and has improved our understanding of past environments and precipitation regimes [12–14].

The δ^2H values of individual lipid biomarkers are particularly useful in paleoenvironmental studies. In particular, the correlation of lipid δ^2H with source water δ^2H has been widely documented [12,15,16], such that leaf waxes are now widely used to reconstruct past hydrological conditions [12,16–18]. Long-chain *n*-alkanes and other non-functionalised hydrocarbons are often used, because they are inherently less susceptible to hydrogen exchange than other compound classes commonly found in sediments, due to their prohibitively high pKas (~ 50). However, a wide range of sedimentary lipids have been analysed for their stable hydrogen isotopic composition, including *n*-alkanes, fatty acids, alkenones, and, to a lesser extent, sterols and hopanols [19–23].

The routine and rapid compound-specific δ^2H value determination of biomarkers (as opposed to labour intensive approaches requiring compound isolation and purification) requires the application of gas chromatography, coupled to an in-line reactor containing active graphite, converting individual organic compounds into CO and H_2 [21,24–27]. The produced gas is introduced into a mass spectrometer detecting m/z 2 (H-H) and 3 (H-D). This setup requires analytes to be GC-amenable [28], limiting analyses to compounds of a molecular weight and polarity low enough to elute at a typical maximum capillary column

operating temperature of 320 °C. Therefore, only very few larger compounds (eluting later than a C_{36} *n*-alkane on an apolar stationary phase) have had their δ^2H values successfully determined. Existing measurements were achieved by implementing long isothermal holds at 320 °C but only with highly purified and ^2H-labelled compounds [29], due to the low GC resolution and δ^2H precision associated with this methodology.

However, the δ^2H values of large and/or polar compounds can be of significant interest. For example, the origin of vegetable oils and milk products can be constrained [30–32] with greater specificity when isotopic fingerprinting is based on individual fatty acids instead of bulk organics [33,34]. Moreover, determining the δ^2H values of intact triacylglycerides (TAG, Suppl. Fig. 1A), instead of hydrolysed and derivatised fatty acids, could have many benefits such as eliminating derivatisation biases and increased specificity. TAG are routinely characterised in food forensics by high temperature gas chromatography (HTGC; Buchgraber et al., 2004; Fontecha et al., 2006; Ruiz-Samblas et al., 2015), but their ^2H signatures are yet to be exploited. Another potential application arises from very long-chain *n*-alkanes that are major constituents of crude oil; their δ^2H values could be used to assess source rock potential [17,18,38,39], or for correlating different oils and source rocks [38,40].

A third suite of applications centres on glycerol dialkyl glycerol tetraether lipids (GDGTs, Suppl. Fig. 1BC), derived from both Archaea and Bacteria and of wide interest in geochemistry. These membrane lipids are frequently used in proxies for paleotemperature and other environmental variables (reviewed in Schouten et al., 2013). In many sedimentary archives, GDGTs are of mixed origins (e.g. De Jonge et al., 2014; Peterse et al., 2009), and their δ^2H values could thus be used to distinguish terrigenous from in situ-produced GDGTs, for example in marine and lacustrine sediments. This would substantially improve the application of these GDGT-based proxies. Moreover, in single-source environments, the hydrogen isotopic composition of GDGTs could serve as a paleohydrological proxy, enabling reconstruction of salinity, elevation, or precipitation. More recently, it has been shown that δ^2H values of bacterial lipids document the metabolic state of the source organisms,

potentially representing another application in biogeochemical investigations (Wijker et al., 2019), and this method will allow to extend such investigations to Archaea.

In order to determine the stable isotopic composition of some of these large molecules, they are often subjected to chemical degradation, and only fragments (mostly aliphatic moieties) that are more GC-amendable than the parent molecule are analysed by GC-IRMS. For TAGs, this involves acid methanolysis [44]. For GDGTs, this involves ether cleavage, followed by reduction [45–50], often including laborious preparative HPLC steps for cleaning and preconcentration [51]. Aside from being labour intensive, such procedures under acidic conditions can result in hydrogen exchange.

However, recently, high temperature GC methods for more direct analysis of these compounds have been developed; identification and quantification of GDGTs has been achieved employing HTGC coupled to time-of-flight mass spectrometry (HTGC-TOFMS) and flame ionisation detection (HTGC-FID [52,53]). Here, we develop these methods further and demonstrate δ^2H analysis of polar and high molecular weight compounds by high temperature gas chromatography coupled to pyrolysis isotope ratio mass spectrometry (HTGC-P-IRMS). We compare the values of purchased, authentic standards (TAGs), and purified standards (GDGTs) determined by elemental analyser pyrolysis isotope ratio mass spectrometry (EA-P-IRMS) with the values determined by HTGC-P-IRMS. We then report the δ^2H values of GDGTs in a number of environmental samples.

Experimental

Standards and environmental samples

Triacylglyceride [trimyristin (C_{42}), tripalmitin (C_{48}), and tristearin (C_{54})] and *n*-alkane standards were purchased from Sigma Aldrich (Gillingham, UK). isoGDGT-2 and isoGDGT-3 standards were purified from biomass of *Sulfolobus solfataricus* (DSM 1616), which was grown in two batches (2 L each) of modified Allen medium [54] using water with a δ^2H value of -55.0 ± 0.2 ‰. Each batch was inoculated with 20 ml of a late log-phase culture, incubated

aerobically at 76 °C with agitation at 200 RPM, and harvested in mid-log phase at an optical density of 0.442 (600 nm). Cells were collected by centrifugation at 4 °C, frozen in liquid nitrogen, and freeze-dried. 0.5 g of the freeze-dried cell pellet was subjected to acid hydrolysis in 5 mL of 1.5 N methanolic HCl (10 % H_2O), and lipids were extracted by ultrasonication in dichloromethane:methanol (1:1; *v/v*) as previously described [55]. The total lipid extract (TLE) was dried under a stream of N_2, dissolved in 1 mL of *n*-hexane: isopropanol (97:3; *v/v*), and filtered through a 0.45 µm PTFE filter.

Individual isoprenoidal GDGTs containing 2 and 3 cyclopentyl moieties (isoGDGT-2 and isoGDGT-3) were isolated by preparative normal phase (NP) high-performance liquid chromatography (HPLC). To this end, aliquots (25 µL) of the filtered TLE were injected onto an Agilent 1100 HPLC system fitted with an Econosphere NH_2 column (250 × 10 mm, 10 µm; Grace/Alltech). GDGTs were eluted isocratically with a solvent mixture of 1.35 % isopropanol (IPA) in *n*-hexane at a flow rate of 1 mL min^{-1} for 45 min, and the column was cleaned with 16 % IPA for 12 min and re-equilibrated to initial conditions for 13 min after every run. GDGTs were recovered by time-based fraction collection, according to the elution times determined by atmospheric pressure chemical ionisation-mass spectrometry (APCI-MS) using an Agilent 1100 MSD [56]. The collected fractions were analysed by flow injection analysis-mass spectrometry on the same instrument, and subsequently pooled by compound. The purity of each isolated GDGT was >97 % as assessed by NP and reverse phase HPLC-ACPI-MS analysis of the combined fractions [57], scanning the range *m/z* of 350–1350.

Environmental samples analysed included a sediment sample from a marine methane seep, and a sample from a Welsh peat [52]. In order to improve gas chromatographic performance, GDGTs were purified prior to HTGC-P-IRMS. The Welsh peat extract was passed over a column containing 130-270 mesh silica (pore size 60 Å 288608, Sigma Aldrich, Gillingham, UK) conditioned in methanol, using two column volumes of each hexane, ethylacetate/hexane 1:9 (v/v), 25:75, 50:50, pure ethylacetate, and methanol.

Concentrations of GDGTs in the fractions were confirmed by adding triglyceride quantification standards and analysis by HTGC-FID [52]. All fractions containing GDGTs (Suppl. Fig. 2) were combined to avoid any isotope fractionation which may have occurred during column chromatography.

^{2}H analysis by EA-P-IRMS

The $^{2}H/^{1}H$ ratios of the triacylglycerides (TAGs) and C_{50} and C_{60} *n*-alkanes were analysed by EA-P-IRMS at Elementar UK Ltd (EUK; Stockport, UK) and University of Colorado (CUB; Boulder, USA). CUB also analysed GDGTs. CUB performed EA-P-IRMS analysis on a Flash HT Plus elemental analyser with zero blank autosampler coupled to a Delta V Plus IRMS via ConFlo-IV Interface (Thermo Scientific). At EUK, EA-P-IRMS measurements were performed using a GeovisION, which comprised a vario PYRO cube coupled to an isoprime visION IRMS. Both laboratories measured samples using glassy carbon reactors in oxygen-free environments, and performed multipoint calibrations using reference materials provided by Arndt Schimmelmann (Indiana University, Bloomington, IN, USA) in order to standardise determined $\delta^{2}H$ values against the international reference Vienna Standard Mean Ocean Water (VSMOW). CUB calibrated using 5α-androstane #3 (-293.2 ± 1.0 ‰), eicosanoic acid methyl ester #Z1 / USGS 70 (-183.9 ± 1.4 ‰), and eicosanoic acid methyl ester #Z2 / USGS 71 (-4.9 ± 1.0 ‰), and EUK calibrated using tetracosane #1: -53.0 per mil ± 1.6 ‰, pentacosane #4: -263.6 ± 2.2 ‰ and heptacosane #3: -172.80 ± 1.6 ‰, and a standard provided by the International Atomic Energy Agency, Vienna (IAEA CH-7: -100.2 ± 1.0 ‰). Across both labs, the standard deviation (SD) of triplicate sample analyses was typically < ±0.75 ‰.

Because the oxygen-bound H atoms of the GDGTs' hydroxyl moieties are easily exchanged, the ^{2}H content at these positions may have been altered during solvent extraction/evaporation. We therefore vapour-equilibrated the dried GDGT fractions with local deionised water (-121.8 ± 1.3 ‰) before analysis (24 h at 25 °C). GDGT fractions were then dissolved in ethyl acetate at ~10 μg μL^{-1} and 10 μL aliquots were pipetted into combusted

(450 °C, 10 h) silver capsules (4x6 mm), which were pre-loaded with small discs (d = 4 mm) of combusted glass fibre filters (Whatman GF/F) as a solvent adsorbent. The solvent was then completely evapourated in a closed chamber continuously purged with N_2 (30 min at ~30 mL min^{-1}). Analysis by EA-P-IRMS was then conducted as described above.

To test for the efficiency of the vapour equilibration, a synthetic diglycerol-trialkyl-tetraether (C_{46}-GTGT; Patwardhan and Thompson, 1999) was exposed to vapour of both ^{2}H-enriched water (7 atom % ^{2}H) and local deionised water (24 h at 25 °C). Exposure to ^{2}H-enriched water vapour increased the ^{2}H content of the molecule by 0.1 atom % (from 0.014 to 0.113 atom % relative to total H), corresponding to a ^{2}H content of ~5 atom % at the OH positions after exposure (assuming all exchange is localised to the hydroxyl moieties). Exposure to natural water vapor, however, did not lead to a change in δ^2H within analytical precision of the measurement. The induced ^{2}H content at the OH positions decreased again to a ^{2}H content of ~2 atom % at the OH-positions after a 12 h exposure to ambient lab air. Together this indicates that OH-bound H of diglycerol tetraethers is readily exchanged with ambient water vapor, and any ^{2}H enrichment resulting from the evaporation of OH-containing solvents (e.g. methanol) were likely diminished either by spontaneous re-equilibration with ambient air, or by the latest through 24 h exposure to natural water vapor in a desiccator as described above.

δ^2H value determination by high-temperature GC-P-IRMS

Before analysis by HTGC-IRMS, fractions containing GDGTs and the sample from the Black Sea methane seep were dissolved in 50 µl pyridine and derivatised to trimethylsilylethers with 50 µl 99% N,O-Bis(trimethylsilyl)trifluoroacetamide *(*BSTFA), 1% trimethylchlorosilane (TMCS), for one hour at 70 °C. The δ^2H value of the TMS moieties used to derivatise the hydroxyl-groups (δ^2H_{TMS}) was determined by derivatisation of sodium palmitate δ^2H_P of a known δ^2H, and analysis by GC-IRMS to yield the values of derivatised palmitate δ^2H_{TMSP}, as -82.35 ‰ acc. to Eqn. 1.

$$\delta^2 H_{TMS} = \frac{\delta^2 H_{TMSP} \cdot 40 - \delta^2 H_P}{9} \quad \text{(Eqn 1)}$$

Values of derivatised GDGTs $\delta^2 H_{meas}$ were corrected by mass balance to give $\delta^2 H_{GDGT}$ with n representing the number of non-exchangeable hydrogens of the compounds and k the number of TMS groups added (1 for archaeol, 2 for GDGTs and hydroxyarchaeol; Eqn. 2).

$$\delta^2 H_{GDGT} = \frac{\delta^2 H_{meas}(n + \mathrm{k} \cdot 9)}{n} - \frac{\mathrm{k} \cdot 9 \cdot \delta^2 H_{TMS}}{n} \quad \text{(Eqn 2)}$$

This was combined into Eqn. 3.

$$\delta^2 H_{GDGT} = \frac{\delta^2 H_{meas}(n + \mathrm{k} \cdot 9)}{n} - \frac{\mathrm{k} \cdot 40 \cdot \delta^2 H_{TMSP}}{n} + \frac{\mathrm{k} \cdot 31 \cdot \delta^2 H_P}{n} \quad \text{(Eqn 3)}$$

Errors of $\delta^2 H_{meas}$ were determined according to error propagation laws:

$$\sigma^2_{\delta^2 H_{GDGT}} = \sigma^2_{\delta^2 H_{meas}} \cdot \left(\frac{n + \mathrm{k} \cdot 9}{n}\right)^2 + \sigma^2_{\delta^2 H_{TMSP}} \cdot \left(\frac{\mathrm{k} \cdot 40}{n}\right)^2 + \sigma^2_{\delta^2 H_P} \cdot \left(\frac{\mathrm{k} \cdot 31}{n}\right)^2 \quad \text{(Eqn 4)}$$

Samples were screened by HTGC-FID as described by Lengger et al. [52] before they were analysed by an Elementar isoprime visION HTGC-P-IRMS (Elementar UK Ltd., Cheadle, UK). The instrument comprised an Agilent 7890B GC fitted with an on-column injector, linked to a GC5 interface (maintained at 380 °C) and a hollow ceramic reactor, enabling pyrolysis at 1450 °C. Ferrules used to connect the ceramic furnace and GC-column, as well as the sample line He used as an additional carrier in the GC-IRMS system, were 100% graphite. Ion beams at *m/z* 2 and 3 were monitored via an isoprime visION mass spectrometer. The H_3^+ factor was determined daily or at least every 4 runs. Compounds were separated on a Zebron ZB-5HT analytical column (7 m × 0.25 mm × 0.1 µm) with high-temperature resistant polyimide coating, which was fitted to a transfer line and an exhaust to allow diversion of the solvent peak to waste via a glass Y-splitter fixed with high temperature resin (Phenomenex Ltd., Aschaffenburg, Germany). He was used as a carrier gas at a flow rate of 2.2 ml min^{-1} ,

and the oven was programmed as follows: 1 min hold at 70 °C, increase by 10 °C min^{-1} to 350 °C, followed by an increase at 3 °C min^{-1} to 400 °C (10 min hold). Results were calibrated using a mixture of *n*-alkanes (B3, A. Schimmelmann, Indiana University, Bloomington, IN, USA) according to Sessions et al. [21,59], which was injected at least every four analyses, and analysed using a He flow of 1 ml min^{-1}, with a different temperature program (injection at 50 °C held for 1 min followed by an increase of 10°C min^{-1} to 300 °C and a 10 min hold). Resultant calibrated δ^2H values were calculated based on the derived linear regression. Root mean standard errors of normalised values of the *n*-alkanes mixture were typically between 4 and 6 ‰, and never exceeded 10 ‰. Data was processed using ionOS stable isotope data processing software (Elementar UK Ltd., UK), using an automated multi-point linearisation based on the certified values of the 15 individual *n*-alkanes comprising the B3 standard.

The fractionation factor $\varepsilon_{H2O/GDGT}$ was determined from the δ^2H_{H2O} and the δ^2H_{GDGT} (Eqn. 5).

$$\varepsilon_{H2O/GDGT} = \left(\frac{\delta_{H2O} + 1}{\delta_{GDGT} + 1} - 1\right) \cdot 1000 \quad \text{(Eqn. 5)}$$

Results and discussion

Chromatographic resolution

The modifications of the GC-IRMS setup enabled operating temperatures of up to 400 °C. Utilisation of a 7-m column and on-column injection enabled elution of isoGDGTs up to GDGT-3, as well as acceptable values for the B3 standard. The GC-IRMS required a polyimide-coated column rather than the metal column commonly employed in high temperature GC-methodologies, as this allowed flow diversion via a glass Y-splitter in which the column was secured using high temperature resin. The glass Y-splitter ensured minimal thermal mass. Furthermore, the pneumatically operated heart-cut valve enabling diversion of the solvent away from the furnace reactor was moved to a location outside of the GC-oven in

order to avoid potential leaks associated with the high temperatures. Methods employing 15 and 30 m polyimide-coated capillary columns, equivalent to the metal columns that had been successfully used to analyse isoGDGTs by HTGC-FID and HTGC-TOFMS at extended > 400 °C isothermals, could not be employed to elute isoGDGTs in analogous HTGC-P-IRMS analyses due to their comparatively low stability at these temperatures.

The unusual HTGC configuration, with a short 7 m column, high flow, and on-column injector, was tested by analysing a mixture of 15 *n*-alkanes: the so-called Indiana B-standard mix routinely used for standardisation of GC-IRMS results. Baseline separation of individual *n*-alkane peaks and acceptable root mean square errors were achieved with this method (Fig. 1A): this standard was subsequently used for quality control and isotope calibration. Root mean square error (RMSE) and linearisation equations for all analyses of the standards are given in Supplementary Fig. 3 and Table 1, with linearisation applied to the samples based on the most contemporary analysis of the standard. RMSE for all accepted analyses were always below 10 ‰: whenever 10 was exceeded, inlet maintenance or column changes were performed. An *n*-alkane standard containing higher molecular weight compounds (up to C_{60}, Fig. 1B), a mixture of triacylglycerides (Fig. 1C), a seep sample containing GDGT-0, -1. -2, and -3, and the two GDGT standards (GDGT-2 and -3) (Fig. 1D) were analysed and chromatograms were similar to previous results employing HTGC-FID and a 7 m column [52]. The brGDGTs eluted earlier than isoGDGTs (cf. [52]).

Accuracy and precision of δ^2H values of high molecular weight compounds

Purchased triaglyceride (TAG) reference compounds and purified GDGT standards were used to test the methodology for accuracy by determining the δ^2H values of these compounds by HTGC-IRMS at GC temperatures of up to 400 °C as well as by EA-analysis. The prepared isoGDGT-2 and isoGDGT-3 standards were analysed by one laboratory (CU Boulder), while the purchased standards were examined by EA-P-IRMS in two different laboratories (CU Boulder and Elementar UK Ltd). The average δ^2H values determined for the TAGs were within 5 ‰ for all analyses (Tab. 1, Fig. 2). HTGC-analysed samples

generally yielded δ^2H values between the values determined by the EA analyses. Standard deviations were smaller for the EA methods (< 2 ‰) than for the HTGC method (9-18 ‰, which represents 2-3× the typical precision of δ^2H value determinations by GC-IRMS; Sessions, 2006). However, here injection concentrations varied, which likely contributed to the variability, which we investigate further below. It is expected that further application of this technique – and routine analysis of TAGs, as compounds of particular interest to the alimentary industry – will lead to improvements in analytical precision as methods are improved by optimising solvents, injection temperatures, and concentrations. The δ^2H values determined for the high molecular weight *n*-alkanes with 50 and 60 carbon atoms (Table 1) were more variable among all methods and laboratories. This was surprising, and possibly a result of insufficient mixing of these large waxy compounds before distribution.

The δ^2H values of purified GDGTs obtained by EA-P-IRMS and HTGC-IRMS (Tab. 1) were not significantly different for GDGT-2 at a high confidence level (Welsh's t-test, df = 2, t = 1.32, p = 0.32). However, for GDGT-3, which eluted later, the δ^2H value derived by HTGC-IRMS was 9 ‰ higher than the value determined by EA-P-IRMS (df = 2, t = 3.32, p = 0.080). A raised baseline could be a possible cause for this discrepancy, but ionOS software applies an automated correction, and both GDGTs eluted on an isothermal baseline. A more likely cause could be fractionation due to chromatographic separation, to adsorption cold spots, or thermal decomposition. Another possibility is minor contamination of GDGT-3, resulting in a flawed EA-P-IRMS measurement but not affecting HTGC-P-IRMS measurements; however, this would be surprising as GDGT-2 and GDGT-3 were isolated from the same organism and the EA-P-IRMS results match expectations of similar δ^2H values. The standard deviation of 5 – 6 ‰ achieved for purified GDGTs using the HTGC-P-IRMS system is similar to the precision of lower molecular weight compounds on a conventional GC-P-IRMS instrument (e.g. Sessions, 2006).

Response vs accuracy

Whilst GDGTs are ubiquitous, they are typically only present at ppm to ppb concentrations in environmental samples such as sediments and soils. In addition, many high molecular weight compounds are not very soluble in solvents suitable for GC-IRMS, and on-column injection only allows small amounts of sample to be used. Therefore, only small amounts of GDGT (ng) were injected for each HTGC-IRMS analysis. To assess accuracy in relationship to signal intensity, different concentrations of the TAG standard were tested and compared to peak heights (Fig. 3). This yielded a response of 0.07 – 0.08 nA per ng H per compound for *m/z* 2. Below ~0.25 nA peak height, values begin to deviate substantially (by ~20 ‰) from the values measured by EA-P-IRMS, with differences of up to 400 ‰ when peak heights were around 0.1 nA. We thus excluded peak heights < 0.25 nA, corresponding to less than 3.5 ng H injected on column. Typical H amounts required to achieve 3-5 ‰ precision were ~10 ng, translating to *m/z* 2 peak heights of 0.7 – 0.8 nA (equivalent to 700-800 mV on an IRMS with a 10^9 Ohm resistor on the operational amplifier for the *m*/*z* 2 faraday cup).

GDGTs in environmental samples and $\varepsilon_{H2O/isoGDGT}$

A sample from a Mediterranean cold seep [52] was analysed, and δ^2H values for archaeol, hydroxyarchaeol, GDGT-1, and GDGT-2 were determined to be -245 ± 7, -253 ± 13, - 216 ± 15, and -225 ± 14, respectively (n=3; Fig. 1D, Fig. 4). These values show a limited range, as expected for ether lipids derived from a common archaeal source, and are similar to published δ^2H values of the biphytanes of GDGTs in *Sulfolobus sp.* determined after ether cleavage (-229 to -257 ‰ [45]). However, the values are not identical, with the diphytanyl glycerol diether lipids archaeol and hydroxyarchaeol being ^2H-depleted relative to GDGTs. Though the difference is small, it could potentially reflect different archaeal origins, given that ANME-2 group Archaea appear to preferentially produce GDGTs in cold seep settings (e.g., Blumenberg et al., 2004); this would be particularly true if the differing source Archaea exhibit different metabolisms (see below).

The $\varepsilon_{H2O/GDGT}$ for the *Sulfolobus* cultures used to purify the standards was determined as -134 ‰ and was lower than previously reported $\varepsilon_{H2O/GDGT}$ (-213‰ to -161‰ [45]). The

application of this fractionation factor to the environmental iso-GDGTs would result in an unrealistic δ^2H value for the seawater of -93 ‰, suggesting that metabolism, salinity, temperature, and other factors contribute strongly to the extent of fractionation.

Values for GDGT-0 from the peat (Suppl. Fig. 4) were similar to the isoGDGTs in the seep sample (-235 ± 3 ‰, n = 2), whereas values for brGDGTs were relatively enriched in ^2H (-176 ± 6 ‰, n = 6). It is possible that the ^2H-enrichment of brGDGTs relative to co-occurring isoGDGTs could be due to fractionation associated with the biosynthetic pathways for isoprenoidal (isoGDGTs) vs. *n*-acyl lipids (brGDGTs), in which isoprenoidal lipids (which undergo successive hydrogenation) exhibit more ^2H-depleted signatures [21,62]. However, recently, it has also been shown that the energy and metabolism pathways of source organisms are highly correlated with δ^2H values of their lipids [63–65]; it is also thought that NADPH/NADH ratios and transhydrogenases play an important role, particularly in anaerobic organisms [66–69]. In general, heterotrophic bacteria consuming TCA-cycle intermediates exhibit δ^2H values similar to or enriched relative to source water, heterotrophs assimilating carbohydrates are slightly depleted relative to source water, and photoautotrophic and chemoautotrophic bacteria show the greatest ^2H-depletion [64]. While Archaea were not examined in this work, some of our results are consistent with the idea that chemoautotrophic archaea are the presumed producers of isoGDGTs in both settings, and heterotrophic bacteria are thought to be the producers of brGDGTs [70].

The differences between the peat and seep samples for isoGDGTs are unexpected: As the δ^2H of the peat water is likely around -52 ‰ [1] – slightly depleted compared to seawater – we expected isoGDGTs from peat to also be depleted in ^2H relative to GDGTs from marine environments. However, isoGDGTs from peat are up to 10 to 20 ‰ more ^2H-enriched in the peat, invoking a difference in metabolic state between the anaerobic methanogens in peat, and the anaerobic methane oxidising communities in the seep. These findings speak to the potential of isoGDGT δ^2H analyses in probing microbial ecology and metabolic state, while

brGDGTs, which are presumably of heterotrophic bacterial origin in peat settings, could prove useful as proxies for source water δ^2H and hydrology.

The novel HTGC-P-IRMS method enables the determination of the δ^2H values of compounds with a high molecular weight, including TAG and GDGT lipids, hereby extending the range of analytes for δ^2H value determination. Accuracy and precision are as small as 3 ‰ in some cases and comparable to EA-P-IRMS. Our initial measurements suggest that bacterial and archaeal GDGT δ^2H values are likely related to both environmental parameters, and the metabolic and ecological function of the source organisms. Future applications include but are not limited to alimentary forensics, archaeology, oil-source rock correlations, microbial ecology and paleoclimate.

Acknowledgements

The authors would like to thank Paul Sutton, Alison Kuhl, Hanna Gruszczynska, Ed Aldred, Xiahong Feng, Alec Cobban, and Michiel Kienhuis for support with measurements, advice, and discussions of techniques. SKL was funded by a Rubicon Grant 825.14.014 from the Netherlands Organisation for Scientific Research (NWO). RDP acknowledges support from ERC (Advanced Grant T-GRES, to RDP). AP and YW acknowledge support from the Swiss National Science Foundation (P2BSP2_168716), and from the Gordon and Betty Moore Foundation and US National Science Foundation (to AP). SHK acknowledges support from the US National Science Foundation. The authors thank the Natural Environment Research Council, UK, for partial funding of the mass spectrometry facilities at Bristol (contract no. R8/H10/63). WDL acknowledges support from the American Chemical Society (PRF 57209-DNI2).

Table 1. δ^2H values determined by EA-IRMS and GC-IRMS.

	EA-IRMS (Elementar)			**EA-IRMS (CU Boulder)**			**HTGC-IRMS**		
	Mean	**St. dev.**	**N**	**Mean**	**St. dev.**	**N**	**Mean**	**St. dev.**	**N**
	[‰ V-SMOW]			[‰ V-SMOW]			[‰ V-SMOW]		
GDGT-2	-	-	-	-181.61	0.41	3	-186.5	6.4	3
GDGT-3	-	-	-	-182.6	0.19	3	-173.0	5.0	3
C_{42}-TAG	-234.97	0.48	4	-237.97	0.72	3	-232.8	9.2	9
C_{48}-TAG	-219.43	1.76	3	-224.14	0.33	3	-222.9	18.2	7
C_{54}-TAG	-225.85	0.38	4	-228.16	0.7	3	-223.0	11.6	7
***n*-C_{60} alk**	-206.49	4.65	3	-213.98	0.35	3	-196.3	2.6	3
***n*-C_{50} alk**	-199.29	0.02	4	-202.05	0.06	3	-187.5	3.0	3

References

1. Bowen GJ, Revenaugh J. Interpolating the isotopic composition of modern meteoric precipitation. *Water Resour Res*. 2003;39(10). doi:10.1029/2003WR002086

2. Craig H. Isotopic Variations in Meteoric Waters. *Science*. 1961;133(3465):1702-1703. doi:10.1126/science.133.3465.1702

3. West JB, Bowen GJ, Dawson TE, Tu KP, eds. *Isoscapes*. Springer Netherlands; 2010. doi:10.1007/978-90-481-3354-3

4. Hobson KA, Wassenaar LI. *Tracking Animal Migration with Stable Isotopes*. Academic Press; 2008.

5. Soto DX, Wassenaar LI, Hobson KA. Stable hydrogen and oxygen isotopes in aquatic food webs are tracers of diet and provenance. *Funct Ecol*. 2013;27(2):535-543. doi:10.1111/1365-2435.12054

6. Fraser I, Meier-Augenstein W. Stable ^{2}H isotope analysis of modern-day human hair and nails can aid forensic human identification. *Rapid Commun Mass Spectrom*. 2007;21(20):3279-3285. doi:10.1002/rcm.3209

7. Schellenberg A, Chmielus S, Schlicht C, et al. Multielement stable isotope ratios (H, C, N, S) of honey from different European regions. *Food Chem*. 2010;121(3):770-777. doi:10.1016/j.foodchem.2009.12.082

8. Chesson LA, Valenzuela LO, O'Grady SP, Cerling TE, Ehleringer JR. Hydrogen and Oxygen Stable Isotope Ratios of Milk in the United States. *J Agric Food Chem*. 2010;58(4):2358-2363. doi:10.1021/jf904151c

9. Chesson LA, Podlesak DW, Erkkila BR, Cerling TE, Ehleringer JR. Isotopic consequences of consumer food choice: Hydrogen and oxygen stable isotope ratios in foods from fast food restaurants versus supermarkets. *Food Chem*. 2010;119(3):1250-1256. doi:10.1016/j.foodchem.2009.07.046

10. Outram AK, Stear NA, Bendrey R, et al. The Earliest Horse Harnessing and Milking. *Science*. 2009;323(5919):1332-1335. doi:10.1126/science.1168594

11. Reynard LM, Hedges REM. Stable hydrogen isotopes of bone collagen in palaeodietary and palaeoenvironmental reconstruction. *J Archaeol Sci*. 2008;35(7):1934-1942. doi:10.1016/j.jas.2007.12.004

12. Sachse D, Billault I, Bowen GJ, et al. Molecular Paleohydrology: Interpreting the Hydrogen-Isotopic Composition of Lipid Biomarkers from Photosynthesizing Organisms. *Annu Rev Earth Planet Sci*. 2012;40(1):221-249. doi:10.1146/annurev-earth-042711-105535

13. Schefuß E, Schouten S, Schneider RR. Climatic controls on central African hydrology during the past 20,000 years. *Nature*. 2005;437(7061):1003-1006. doi:10.1038/nature03945

14. Tierney JE, Russell JM, Huang Y, Damsté JSS, Hopmans EC, Cohen AS. Northern Hemisphere Controls on Tropical Southeast African Climate During the Past 60,000 Years. *Science*. 2008;322(5899):252-255. doi:10.1126/science.1160485

15. Estep MF, Hoering TC. Biogeochemistry of the stable hydrogen isotopes. *Geochim Cosmochim Acta*. 1980;44(8):1197-1206. doi:10.1016/0016-7037(80)90073-3

16. da Silveira Lobo Sternberg L. D/H ratios of environmental water recorded by D/H ratios of plant lipids. *Nature*. 1988;333(6168):59-61. doi:10.1038/333059a0

17. Sessions AL. Review: Factors Controlling the Deuterium Contents of Sedimentary Hydrocarbons. *Org Geochem*. 2016;96:43-64. doi:10.1016/j.orggeochem.2016.02.012

18. Sessions AL, Sylva SP, Summons RE, Hayes JM. Isotopic exchange of carbon-bound hydrogen over geologic timescales. *Geochim Cosmochim Acta*. 2004;68(7):1545-1559. doi:10.1016/j.gca.2003.06.004

19. Li C, Sessions AL, Kinnaman FS, Valentine DL. Hydrogen-isotopic variability in lipids from Santa Barbara Basin sediments. *Geochim Cosmochim Acta*. 2009;73(16):4803-4823. doi:10.1016/j.gca.2009.05.056

20. Sauer PE, Eglinton TI, Hayes JM, Schimmelmann A, Sessions AL. Compound-specific D/H ratios of lipid biomarkers from sediments as a proxy for environmental and climatic conditions. *Geochim Cosmochim Acta*. 2001;65(2):213-222. doi:10.1016/S0016-7037(00)00520-2

21. Sessions AL, Burgoyne TW, Schimmelmann A, Hayes JM. Fractionation of hydrogen isotopes in lipid biosynthesis. *Org Geochem*. 1999;30(9):1193-1200. doi:10.1016/S0146-6380(99)00094-7

22. Smittenberg RH, Sachs JP. Purification of dinosterol for hydrogen isotopic analysis using high-performance liquid chromatography–mass spectrometry. *J Chromatogr A*. 2007;1169(1-2):70-76. doi:10.1016/j.chroma.2007.09.018

23. van der Meer MTJ, Baas M, Rijpstra WIC, et al. Hydrogen isotopic compositions of long-chain alkenones record freshwater flooding of the Eastern Mediterranean at the onset of sapropel deposition. *Earth Planet Sci Lett*. 2007;262(3-4):594-600. doi:10.1016/j.epsl.2007.08.014

24. Burgoyne TW, Hayes JM. Quantitative Production of H_2 by Pyrolysis of Gas Chromatographic Effluents. *Anal Chem*. 1998;70(24):5136-5141. doi:10.1021/ac980248v

25. Hilkert AW, Douthitt CB, Schlüter HJ, Brand WA. Isotope ratio monitoring gas chromatography/Mass spectrometry of D/H by high temperature conversion isotope ratio mass spectrometry. *Rapid Commun Mass Spectrom*. 1999;13(13):1226-1230. doi:10.1002/(SICI)1097-0231(19990715)13:13<1226::AID-RCM575>3.0.CO;2-9

26. Scrimgeour CM, Begley IS, Thomason ML. Measurement of deuterium incorporation into fatty acids by gas chromatography/isotope ratio mass spectrometry. *Rapid Commun Mass Spectrom*. 1999;13(4):271-274. doi:10.1002/(SICI)1097-0231(19990228)13:4<271::AID-RCM468>3.0.CO;2-6

27. Tobias HJ, Brenna JT. On-Line Pyrolysis as a Limitless Reduction Source for High-Precision Isotopic Analysis of Organic-Derived Hydrogen. *Anal Chem*. 1997;69(16):3148-3152. doi:10.1021/ac970332v

28. Kaal E, Janssen H-G. Extending the molecular application range of gas chromatography. *J Chromatogr A*. 2008;1184(1-2):43-60. doi:10.1016/j.chroma.2007.11.114

29. Bodlenner A, Liu W, Hirsch G, et al. C_{35} Hopanoid Side Chain Biosynthesis: Reduction of Ribosylhopane into Bacteriohopanetetrol by a Cell-Free System from Methylobacterium organophilum. *ChemBioChem*. 2015;16(12):1764-1770. doi:10.1002/cbic.201500021

30. Muhammad SA, Seow E-K, Omar AM, et al. Variation of delta H-2, delta O-18 & delta C-13 in crude palm oil from different regions in Malaysia: Potential of stable isotope signatures as a key traceability parameter. *Sci Justice*. 2018;58(1):59-66. doi:10.1016/j.scijus.2017.05.008

31. Richter EK, Spangenberg JE, Kreuzer M, Leiber F. Characterization of Rapeseed (Brassica napus) Oils by Bulk C, O, H, and Fatty Acid C Stable Isotope Analyses. *J Agric Food Chem*. 2010;58(13):8048-8055. doi:10.1021/jf101128f

32. Spangenberg JE. Bulk C, H, O, and fatty acid C stable isotope analyses for purity assessment of vegetable oils from the southern and northern hemispheres. *Rapid Commun Mass Spectrom*. 2016;30(23):2447-2461. doi:10.1002/rcm.7734

33. Ehtesham E, Hayman AR, McComb KA, Van Hale R, Frew RD. Correlation of Geographical Location with Stable Isotope Values of Hydrogen and Carbon of Fatty Acids from New Zealand Milk and Bulk Milk Powder. *J Agric Food Chem*. 2013;61(37):8914-8923. doi:10.1021/jf4024883

34. Paolini M, Bontempo L, Camin F. Compound-specific delta C-13 and delta H-2 analysis of olive oil fatty acids. *Talanta*. 2017;174:38-43. doi:10.1016/j.talanta.2017.05.080

35. Buchgraber M, Ulberth F, Anklam E. Cluster analysis for the systematic grouping of genuine cocoa butter and cocoa butter equivalent samples based on triglyceride patterns. *J Agric Food Chem*. 2004;52(12):3855-3860. doi:10.1021/jf035153v

36. Fontecha J, Mayo I, Toledano G, Juárez M. Use of changes in triacylglycerols during ripening of cheeses with high lipolysis levels for detection of milk fat authenticity. *Int Dairy J*. 2006;16(12):1498-1504. doi:10.1016/j.idairyj.2005.12.005

37. Ruiz-Samblas C, Gonzalez-Casado A, Cuadros-Rodriguez L. Triacylglycerols Determination by High-temperature Gas Chromatography in the Analysis of Vegetable Oils and Foods: A Review of the Past 10 Years. *Crit Rev Food Sci Nutr*. 2015;55(11):1618-1631. doi:10.1080/10408398.2012.713045

38. Pedentchouk N, Turich C. Carbon and hydrogen isotopic compositions of n-alkanes as a tool in petroleum exploration. *Geol Soc Lond Spec Publ*. 2018;468(1):105-125. doi:10.1144/SP468.1

39. Radke J, Bechtel A, Gaupp R, et al. Correlation between hydrogen isotope ratios of lipid biomarkers and sediment maturity. *Geochim Cosmochim Acta*. 2005;69(23):5517-5530. doi:10.1016/j.gca.2005.07.014

40. Li M, Huang Y, Obermajer M, Jiang C, Snowdon LR, Fowler MG. Hydrogen isotopic compositions of individual alkanes as a new approach to petroleum correlation: case studies from the Western Canada Sedimentary Basin. *Org Geochem*. 2001;32(12):1387-1399. doi:10.1016/S0146-6380(01)00116-4

41. Schouten S, Hopmans EC, Sinninghe Damsté JS. The organic geochemistry of glycerol dialkyl glycerol tetraether lipids: A review. *Org Geochem*. 2013;54:19-61. doi:10.1016/j.orggeochem.2012.09.006

42. De Jonge C, Stadnitskaia A, Hopmans EC, Cherkashov G, Fedotov A, Sinninghe Damsté JS. In situ produced branched glycerol dialkyl glycerol tetraethers in suspended particulate matter from the Yenisei River, Eastern Siberia. *Geochim Cosmochim Acta*. 2014;125:476-491. doi:10.1016/j.gca.2013.10.031

43. Peterse F, Kim J-H, Schouten S, Kristensen DK, Koç N, Sinninghe Damsté JS. Constraints on the application of the MBT/CBT palaeothermometer at high latitude environments (Svalbard, Norway). *Org Geochem*. 2009;40(6):692-699. doi:10.1016/j.orggeochem.2009.03.004

44. Correa-Ascencio M, Evershed RP. High throughput screening of organic residues in archaeological potsherds using direct acidified methanol extraction. *Anal Methods*. 2014;6(5):1330-1340. doi:10.1039/C3AY41678J

45. Kaneko M, Kitajima F, Naraoka H. Stable hydrogen isotope measurement of archaeal ether-bound hydrocarbons. *Org Geochem*. 2011;42(2):166-172. doi:10.1016/j.orggeochem.2010.11.002

46. Lengger SK, Lipsewers YA, de Haas H, Sinninghe Damsté JS, Schouten S. Lack of ^{13}C-label incorporation suggests low turnover rates of thaumarchaeal intact polar tetraether lipids in sediments from the Iceland shelf. *Biogeosciences*. 2014;11(2):201-216. doi:10.5194/bg-11-201-2014

47. Schouten S, Hoefs MJL, Koopmans MP, Bosch H-J, Sinninghe Damsté JS. Structural characterization, occurrence and fate of archaeal ether-bound acyclic and cyclic biphytanes and corresponding diols in sediments. *Org Geochem*. 1998;29(5-7):1305-1319. doi:10.1016/S0146-6380(98)00131-4

48. Weber Y, Damsté JSS, Zopfi J, et al. Redox-dependent niche differentiation provides evidence for multiple bacterial sources of glycerol tetraether lipids in lakes. *Proc Natl Acad Sci*. 2018;115(43):10926-10931. doi:10.1073/pnas.1805186115

49. Weber Y, De Jonge C, Rijpstra WIC, et al. Identification and carbon isotope composition of a novel branched GDGT isomer in lake sediments: Evidence for lacustrine branched GDGT production. *Geochim Cosmochim Acta*. 2015;154:118-129. doi:10.1016/j.gca.2015.01.032

50. Wegener G, Bausch M, Holler T, et al. Assessing sub-seafloor microbial activity by combined stable isotope probing with deuterated water and ^{13}C-bicarbonate: Microbial carbon assimilation in the sub-seafloor. *Environ Microbiol*. 2012;14(6):1517-1527. doi:10.1111/j.1462-2920.2012.02739.x

51. Weijers JWH, Wiesenberg GLB, Bol R, Hopmans EC, Pancost RD. Carbon isotopic composition of branched tetraether membrane lipids in soils suggest a rapid turnover and a heterotrophic life style of their source organism(s). *Biogeosciences*. 2010;7(9):2959-2973. doi:10.5194/bg-7-2959-2010

52. Lengger SK, Sutton PA, Rowland SJ, et al. Archaeal and bacterial glycerol dialkyl glycerol tetraether (GDGT) lipids in environmental samples by high temperature-gas chromatography with flame ionisation and time-of-flight mass spectrometry detection. *Org Geochem*. 2018;121:10-21. doi:10.1016/j.orggeochem.2018.03.012

53. Sutton PA, Rowland SJ. High temperature gas chromatography–time-of-flight-mass spectrometry (HTGC–ToF-MS) for high-boiling compounds. *J Chromatogr A*. 2012;1243:69-80. doi:10.1016/j.chroma.2012.04.044

54. Worthington P, Blum P, Perez-Pomares F, Elthon T. Large-Scale Cultivation of Acidophilic Hyperthermophiles for Recovery of Secreted Proteins. *Appl Env Microbiol*. 2003;69(1):252-257. doi:10.1128/AEM.69.1.252-257.2003

55. Weber Y, Damsté JSS, Hopmans EC, Lehmann MF, Niemann H. Incomplete recovery of intact polar glycerol dialkyl glycerol tetraethers from lacustrine suspended biomass. *Limnol Oceanogr Methods*. 2017;15(9):782-793. doi:10.1002/lom3.10198

56. Schouten S, Huguet C, Hopmans EC, Kienhuis MVM, Sinninghe Damsté JS. Analytical methodology for TEX_{86} paleothermometry by High-Performance Liquid Chromatography/Atmospheric Pressure Chemical Ionization-Mass Spectrometry. *Anal Chem*. 2007;79(7):2940-2944. doi:10.1021/ac062339v

57. Smittenberg RH, Hopmans EC, Schouten S, Sinninghe Damsté JS. Rapid isolation of biomarkers for compound specific radiocarbon dating using high-performance liquid chromatography and flow injection analysis–atmospheric pressure chemical ionisation mass spectrometry. *J Chromatogr A*. 2002;978(1):129-140. doi:10.1016/S0021-9673(02)01427-9

58. Patwardhan AP, Thompson DH. Efficient Synthesis of 40- and 48-Membered Tetraether Macrocyclic Bisphosphocholines. *Org Lett*. 1999;1(2):241-244. doi:10.1021/ol990567o

59. Sessions AL, Jahnke LL, Schimmelmann A, Hayes JM. Hydrogen isotope fractionation in lipids of the methane-oxidizing bacterium Methylococcus capsulatus. *Geochim Cosmochim Acta*. 2002;66(22):3955-3969. doi:10.1016/S0016-7037(02)00981-X

60. Sessions AL. Isotope-ratio detection for gas chromatography. *J Sep Sci*. 2006;29(12):1946-1961. doi:10.1002/jssc.200600002

61. Blumenberg M, Seifert R, Reitner J, Pape T, Michaelis W. Membrane lipid patterns typify distinct anaerobic methanotrophic consortia. *Proc Natl Acad Sci*. 2004;101(30):11111-11116. doi:10.1073/pnas.0401188101

62. Zhang Z, Sachs JP. Hydrogen isotope fractionation in freshwater algae: I. Variations among lipids and species. *Org Geochem*. 2007;38(4):582-608. doi:10.1016/j.orggeochem.2006.12.004

63. Osburn MR, Dawson KS, Fogel ML, Sessions AL. Fractionation of Hydrogen Isotopes by Sulfate- and Nitrate-Reducing Bacteria. *Front Microbiol*. 2016;7. doi:10.3389/fmicb.2016.01166

64. Wijker RS, Sessions AL, Fuhrer T, Phan M. $^{2}H/^{1}H$ variation in microbial lipids is controlled by NADPH metabolism. *Proc Natl Acad Sci*. 2019;116(25):12173-12182. doi:10.1073/pnas.1818372116

65. Zhang X, Gillespie AL, Sessions AL. Large D/H variations in bacterial lipids reflect central metabolic pathways. *Proc Natl Acad Sci*. 2009;106(31):12580-12586. doi:10.1073/pnas.0903030106

66. Campbell BJ, Sessions AL, Fox DN, et al. Minimal Influence of [NiFe] Hydrogenase on Hydrogen Isotope Fractionation in H2-Oxidizing Cupriavidus necator. *Front Microbiol*. 2017;8. doi:10.3389/fmicb.2017.01886

67. Dawson KS, Osburn MR, Sessions AL, Orphan VJ. Metabolic associations with archaea drive shifts in hydrogen isotope fractionation in sulfate-reducing bacterial lipids in cocultures and methane seeps. *Geobiology*. 2015;13(5):462-477. doi:10.1111/gbi.12140

68. Leavitt WD, Murphy SJ-L, Lynd LR, Bradley AS. Hydrogen isotope composition of Thermoanaerobacterium saccharolyticum lipids: Comparing wild type with a nfn-transhydrogenase mutant. *Org Geochem*. 2017;113:239-241. doi:10.1016/j.orggeochem.2017.06.020

69. Leavitt WD, Flynn TM, Suess MK, Bradley AS. Transhydrogenase and Growth Substrate Influence Lipid Hydrogen Isotope Ratios in Desulfovibrio alaskensis G20. *Front Microbiol*. 2016;07. doi:10.3389/fmicb.2016.00918

70. Sinninghe Damsté JS, Rijpstra WIC, Foesel BU, et al. An overview of the occurrence of ether- and ester-linked iso-diabolic acid membrane lipids in microbial cultures of the Acidobacteria: Implications for brGDGT paleoproxies for temperature and pH. *Org Geochem*. 2018;124:63-76. doi:10.1016/j.orggeochem.2018.07.006

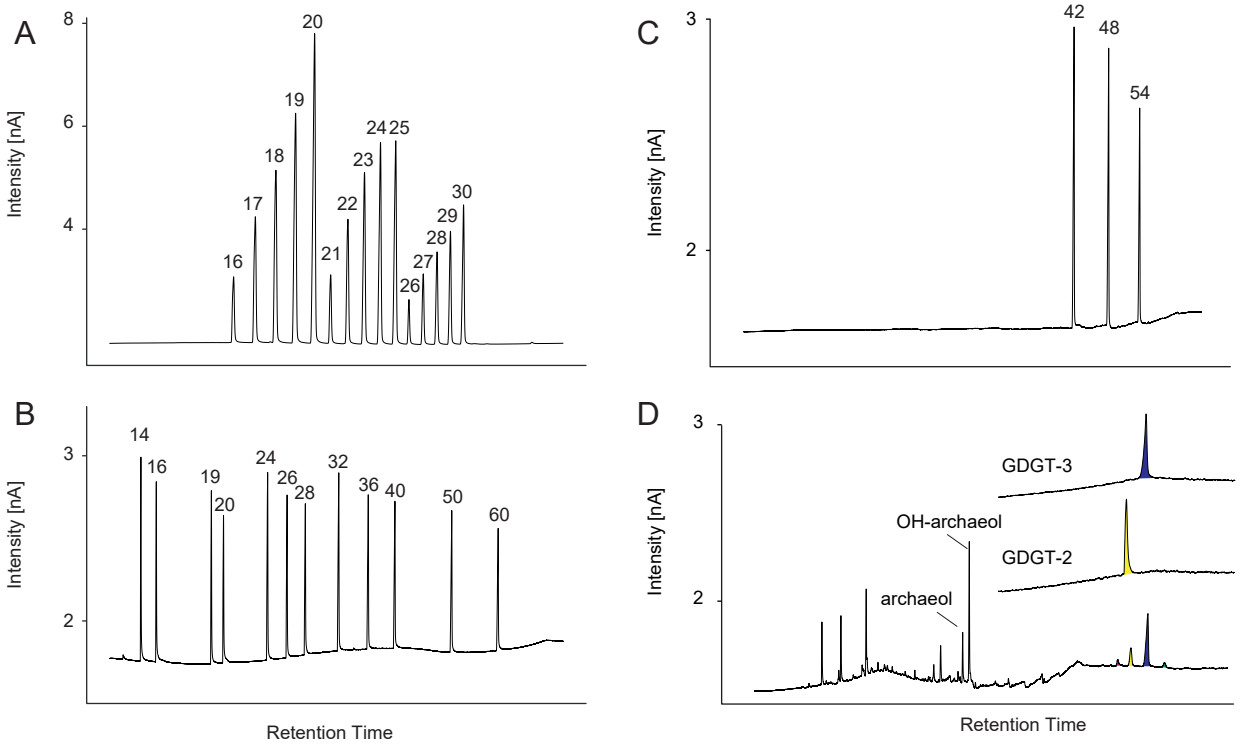

Figure 1. GC-P-IRMS chromatograms under HT conditions, different temperature ramps were applied to the different mixtures. Shown is a mixture of n-alkanes up to n-C30 with known δ2H values (Indiana B3-standard, A), a mixture of long chain n-alkanes up to n-C60 (B), triacylglycerides (C), and a sample from a Black Sea methane seep (D) with GDGT-2 and GDGT-3 standards shown as inserts.

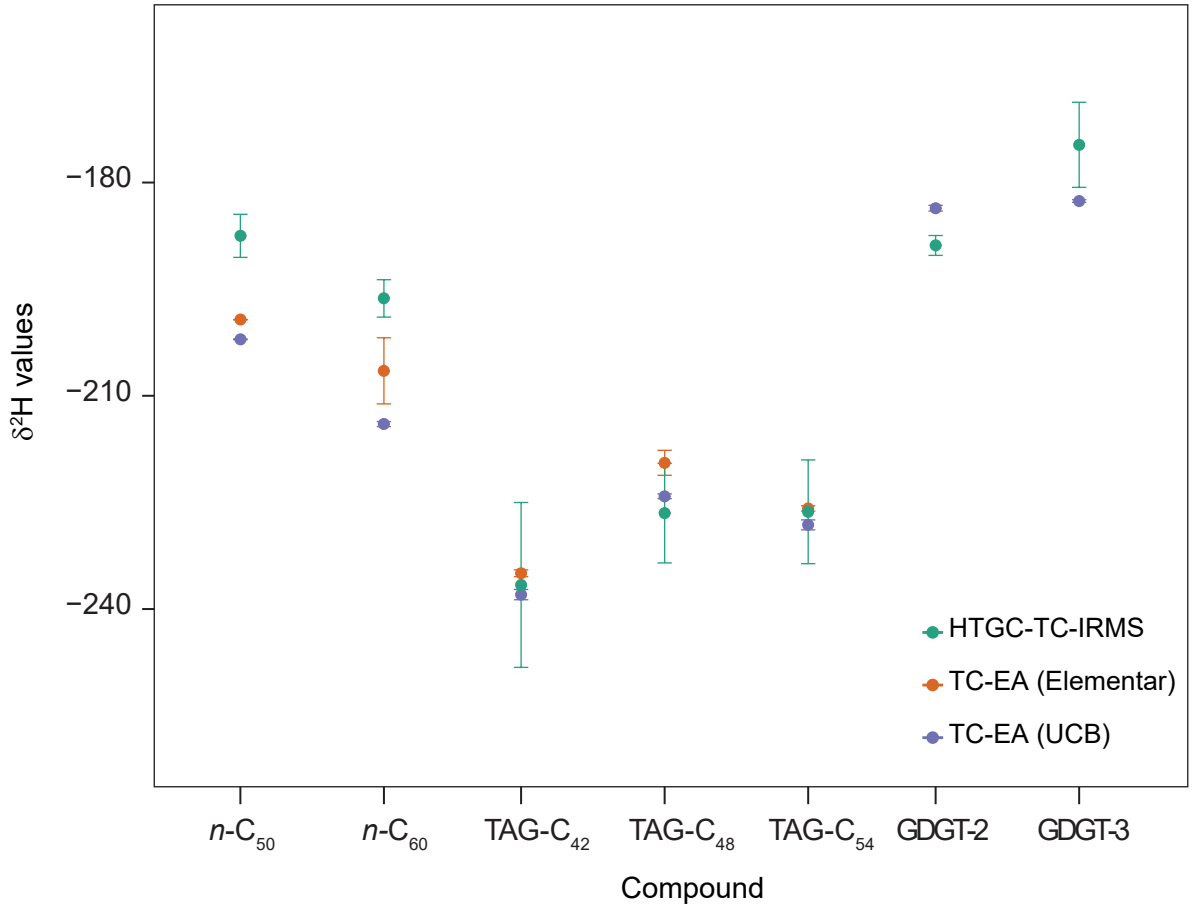

Figure 2. δ2H values of purchased triacylglyceride standards and isolated GDGTs determined by EA-P-IRMS compared with values as determined by HTGC-P-IRMS; values and standard errors are given in Table 1.

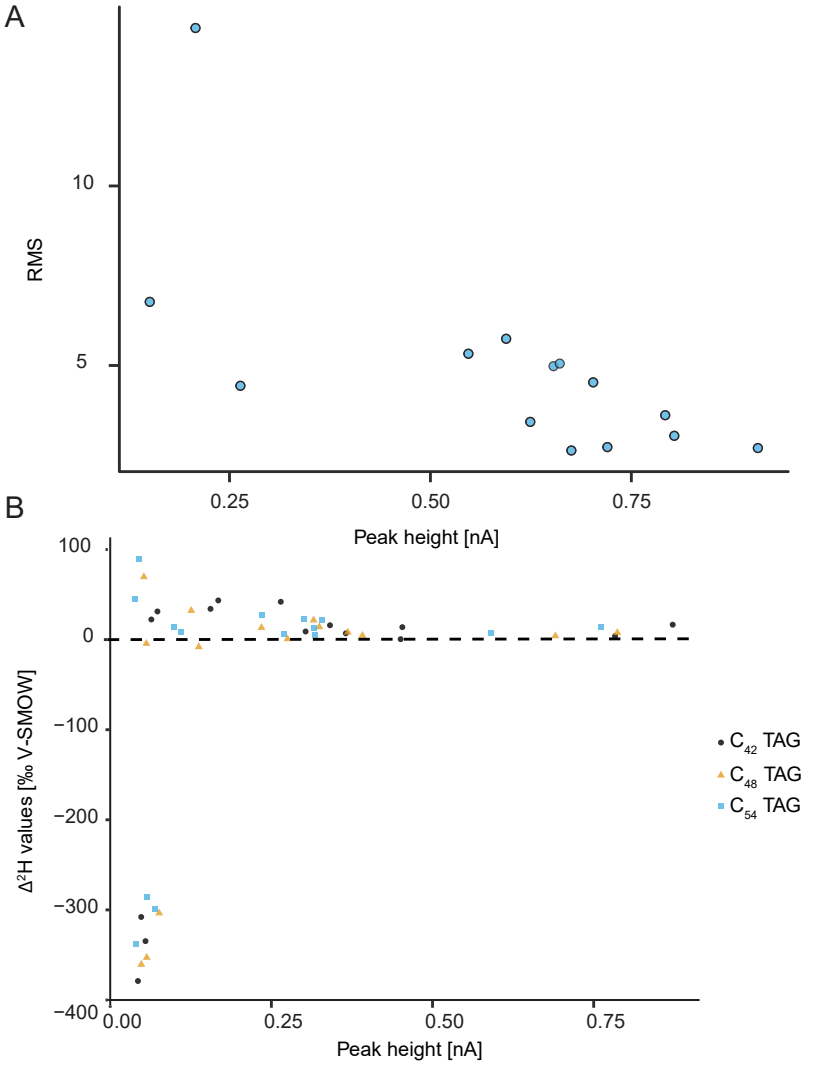

Figure 3. Effect of signal height on δ2H values. A RMSE of the B3 mixture compared to peak heights of the minimum peak height in the mixture. B Difference δ2H values of TAGs determined by HTGC-P-IRMS to values determined by EA-P-IRMS plotted vs peak height.

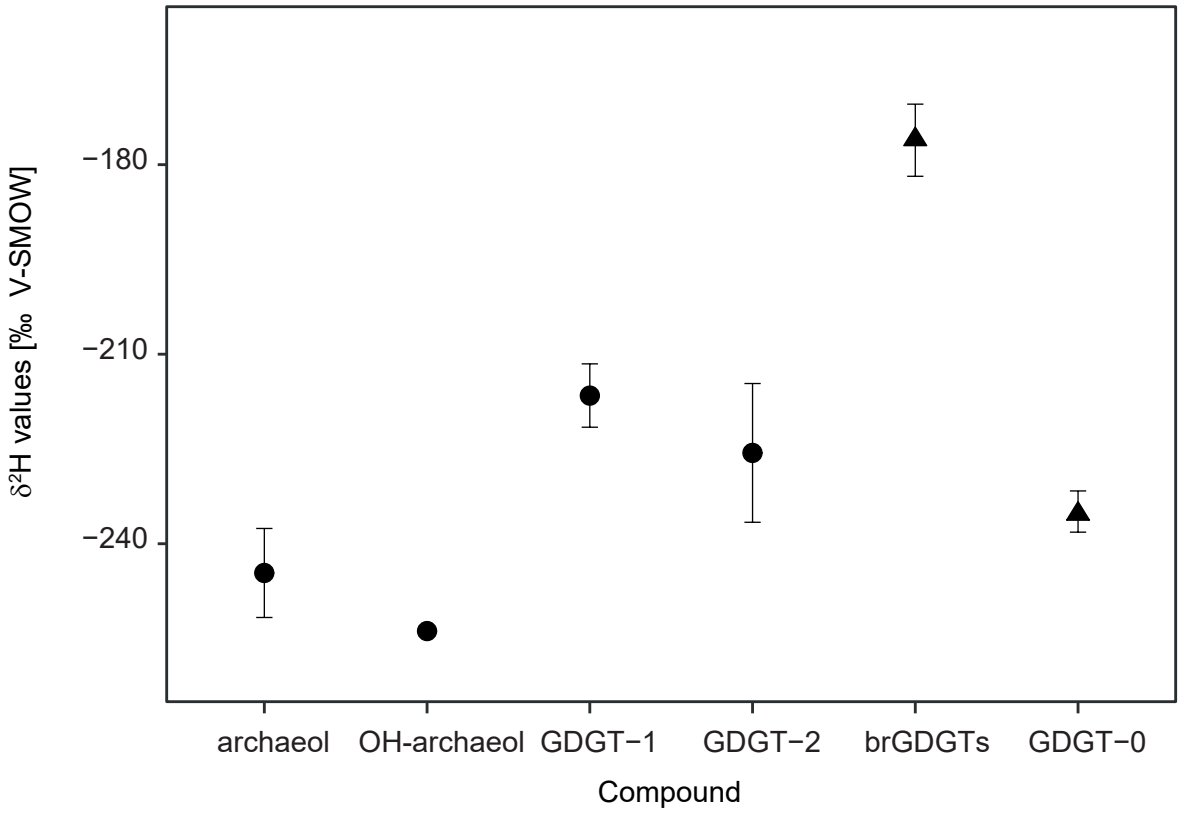

Figure 4. δ2H values of ether lipids determined from environmental samples. brGDGTs and GDGT-0 were extracted from a peat (triangles) and all other compounds derived from a methane seep (circles). Error bars represent standard deviations.

Supplementary to: Determination of the δ^2H values of high molecular weight lipids by high temperature GC coupled to isotope ratio mass spectrometry

Sabine K. Lengger[1,2,*], Yuki Weber[3], Kyle W.R. Taylor[4], Sebastian H. Kopf[5], Robert Berstan[4], Ian D. Bull[1], Jan-Peter Mayser[1], William D. Leavitt[6], Jerome Blewett[1], Ann Pearson[3] and Richard D. Pancost[1,7]

1 Organic Geochemistry Unit, School of Chemistry, University of Bristol, Cantock's Close, Bristol BS81TS, UK

2 Biogeochemistry Research Centre, School of Geography, Earth and Environmental Science, University of Plymouth, Drake Circus, Plymouth PL48AA, UK

3 Department of Earth and Planetary Sciences, Harvard University, 20 Oxford St, Cambridge, MA 02138, USA

4 Elementar UK Ltd., Earl Road, Cheadle Hulme, Stockport, SK8 6PT, UK

5 Department of Geological Sciences, University of Colorado Boulder, Boulder, CO, USA

6 Department of Earth Science, Department of Chemistry, Department of Biological Sciences, Dartmouth College, Hanover, NH, USA

7 School of Earth Sciences and Cabot Institute for the Environment, University of Bristol, Queens Road, Bristol BS81RL, UK

* corresponding author: sabine.lengger@plymouth.ac.uk

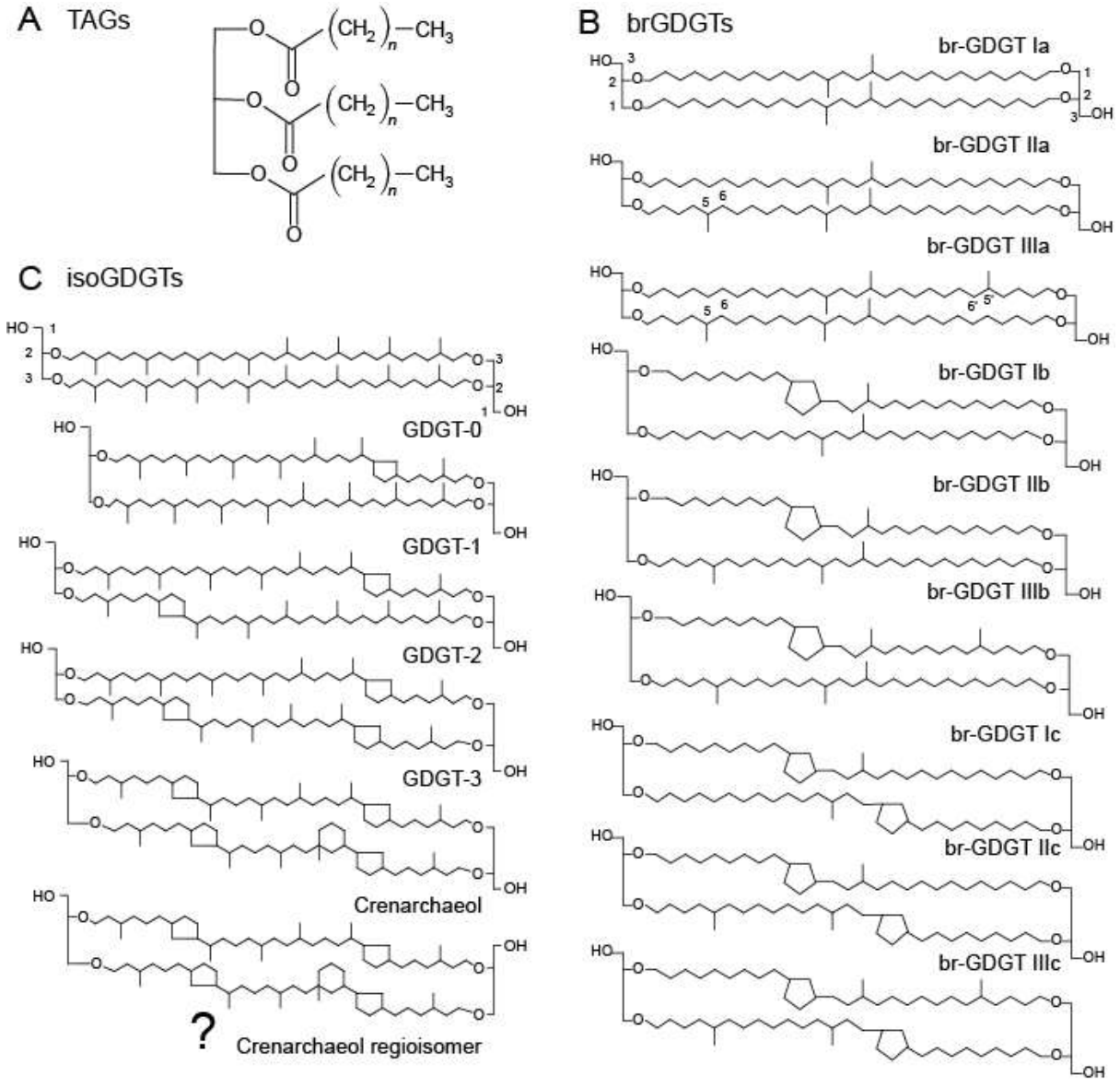

Supplementary Figure 1. Structures of analysed compounds. n = 14 (Trimyristate, C_{42}); 16 (Tripalmitate, C_{48}); 18 (Tristearate, C_{54}).

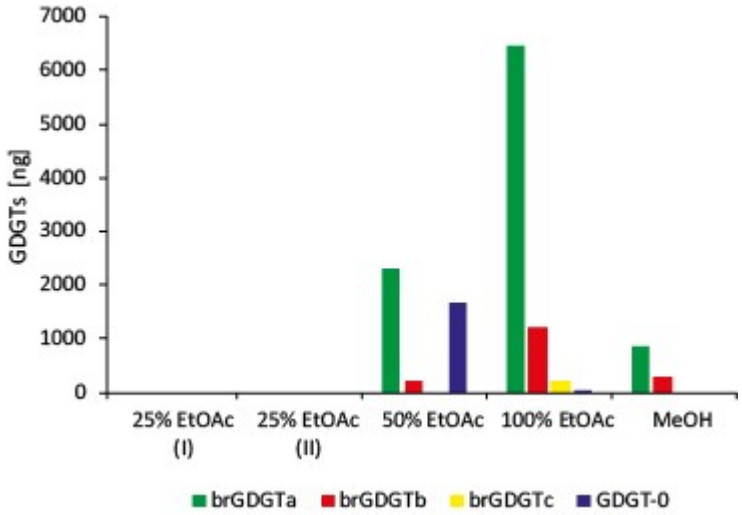

Supplementary Figure 2. GDGTs in column chromatography fractions of sample from a Cors Caron peat (depth 100-200 mm below water table) as determined by HTGC-FID and comparison to triacylglyceride standards as described by Lengger et al. (2018), with a, b and c denoting acyclic, mono-, and bi-cyclic brGDGTs, respectively.

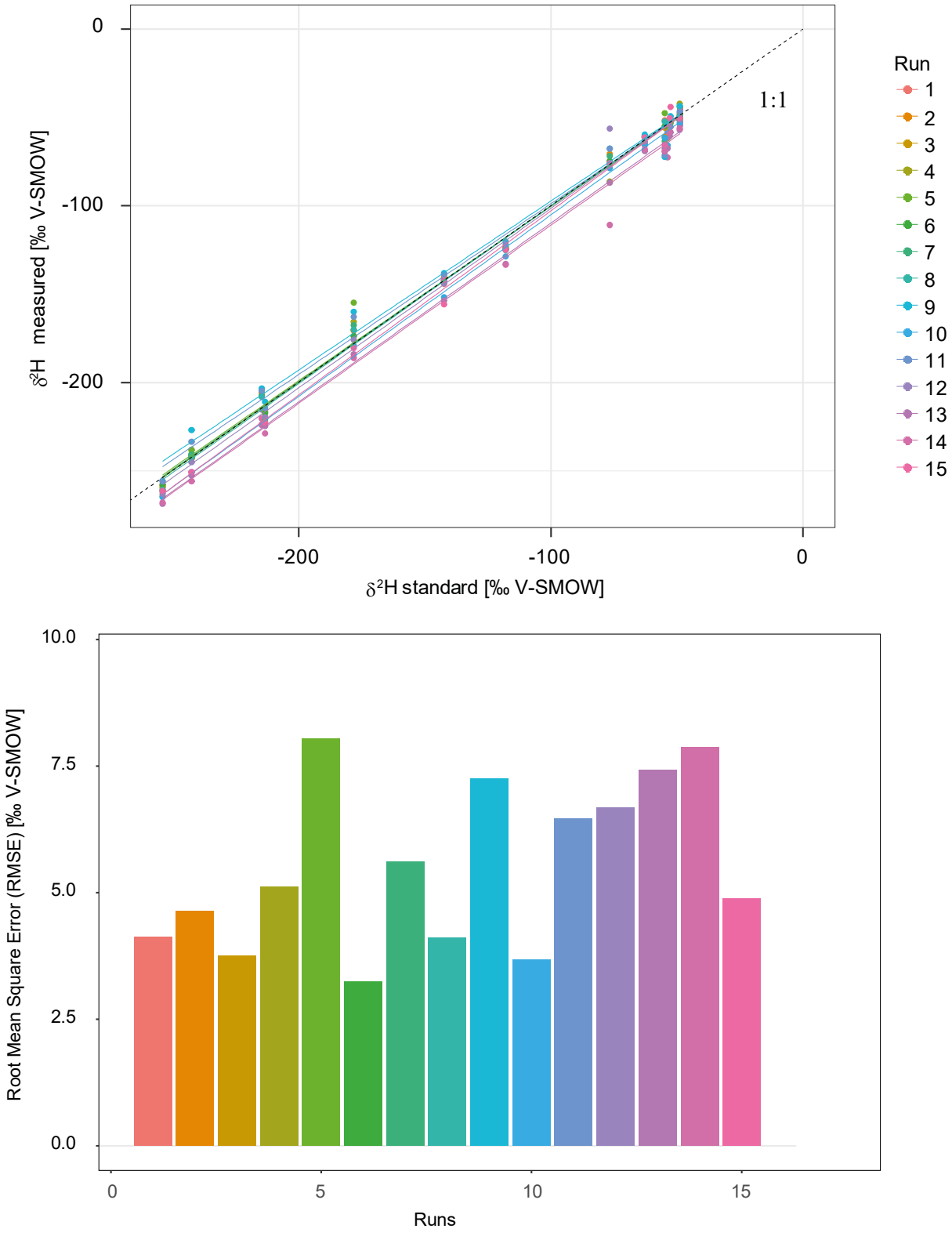

Supplementary Figure 3. Performance monitoring results of *n*-alkane mixture B3 and Root Mean Square Error (RMSE) values of linearisations used for the measurements. Linear regression results and RMSE are shown in table 1.

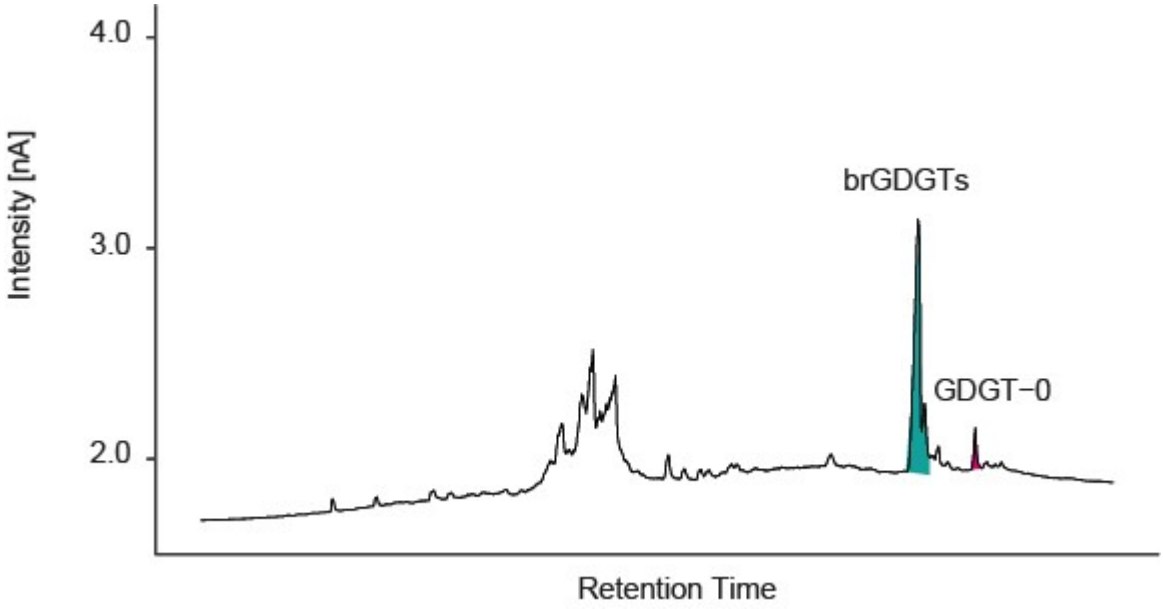

Supplementary Figure 4. Chromatogram of a combined GDGT-fraction from a Welsh peat analysed by HTGC-P-IRMS.

Table S1. Linearisation coefficients and RMSE of B3 standard runs.

Run nr	**Intercept** [‰ V-SMOW]	**Coefficient**	**RMSE** [‰ V-SMOW]
1	-18.3	0.9615	4.1
2	-16.4	0.9629	4.6
3	-20.2	0.9759	3.8
4	-19.4	0.9152	5.1
5	-21.0	0.9120	8.0
6	-18.6	0.9924	3.2
7	-20.1	0.9597	5.6
8	-19.0	0.9703	4.1
9	-21.1	0.9225	7.3
10	-21.9	0.9905	3.7
11	-21.7	0.9319	6.5
12	-19.4	0.9799	6.7
13	-27.7	0.9762	3.0
14	-29.2	0.9730	7.9
15	-18.2	1.0048	4.9